Application of wavelet transform de-noising in pole identification of a system

CHEN Shi-Guo[1,2], ZHANG Ruan-Yu[1], WANG Peng[1], LI Tai-Hua[1]

([1] No.720 Institute of Sichuan University, Key Laboratory for Radiation Physics and Technology of Ministry of Education, Chengdu 610064; [2] Guizhou Normal University, Guiyang 550001)

Abstract Due to the multiscale character of wavelet transform, the method of wavelet transform de-noising (WTDN) is introduced. The WTDN method neither requires extra limit of frequency range for the processed signal, nor needs a prior estimate of impulse response for an identified system, so it is especially suitable to de-noise the wide-band signal and the impulse response of a blind system. The numerical simulation results indicate that the WTDN method is reliable. The WTDN method was used to process the sampled data from a preamplifier coupled to a gas detector. The experimental results also show that the WTDN method can effectively improve the SNR of sampled data and enhance the accuracy in pole identification of the system.

Keywords Wavelet transform, Pole identification, Accuracy, Impulse response

CLC number TL82

1 Introduction

In nuclear spectroscopy, mixed analog-digital filter can approach efficiently the optimal resolution of the instrument.[1-4] To design the digital filter with pole-zero compensation, it is necessary to know accurately the pole positions of the analog filter, which can be implemented by the N4SID (numerical algorithms for subspace state system identification) method.[5-7] With identifying the poles by the N4SID method, the signal-to-noise ratio (SNR) can not be very low in order to avoid that the signal singular values are submerged by noise singular values, otherwise a wrong estimation of poles of an identified system will be made.[6] A preprocessing method to enhance the SNR of the sampled data has been introduced in Ref. [7], which is called as LFDN (low-pass filter de-noising). The LFDN relies on the hypothesis that the signal is bandwidth-limited, and its bandwidth is narrower than that of the corrupting noise. The basic idea of the LFDN is that the difference between the measured impulse response and a prior estimate of the impulse response (which is supposed to be available) is filtered, and successively a new "noise" impulse response, characterized by a higher SNR, is reconstructed. The limitation of the LFDN is that if the frequency band of the impulse response of the identified system is very wide, such as containing high frequency, then the de-noising effect is not ideal. Besides, since an available prior estimate of the identified system is needed, it will be difficult to identify the poles of a blind system.

Wavelet transform is a novel signal processing technique and has been widely used.[8-12] The main characteristic of wavelet transform is that its time-frequency localization or scale is changed in the entire time–frequency domain. Thus, wavelet transform has multiscale characteristic and the scale can be adjusted according to the signal features.[9,10] Therefore, the original signal can be decomposed into a series of localized components depicted by dilation and translation parameters, and each of the components represents the information of different frequency contained in analyzed signals. Based on this characteristic, the method of wavelet transform de-noising (WTDN) is introduced to improve the SNR of sampled data and to enhance the accuracy in pole identification of a system with the N4SID method.

Received date: 2003-09-26

2 Wavelet transform de-noising

Any signal can be decomposed into the components with projecting it on the corresponding wavelet basis function, and every component is related to different region of the time-frequency (or scale) domain. Fast algorithms computing the wavelet decomposition are based on representing the projection of the signal on the corresponding basis function, which resembles a filtering operation.[9,10] Thus, the wavelet transform coefficients of signal $f(n)$ at different scales can be obtained as follows:

$$A_{2^j}\{f(n)\}=\sum_{k=-\infty}^{\infty}h(k)A_{2^{j-1}}\{f(n-k)\} \tag{1}$$

$$D_{2^j}\{f(n)\}=\sum_{k=-\infty}^{\infty}g(k)A_{2^{j-1}}\{f(n-k)\} \tag{2}$$

Succinctly, A^j and D^j are obtained from A^{j-1} by

$$A^j=\sum_k h_{k-2L}A^{j-1} \tag{3}$$

$$D^j=\sum_k g_{k-2L}A^{j-1} \tag{4}$$

where A^j and D^j are j^{th} discrete approximation and discrete detail, and $h(k)$ and $g(k)$ are discrete low-pass filter and discrete high-pass filter.

The reconstructed signal can be presented as

$$A^{j-1}=\sum_k h_{k-2L}A^j+\sum_k g_{k-2L}D^j \tag{5}$$

In the de-noising process, a threshold δ^j is obtained by processing the coefficients D^j with some prior information on signals and noises, and any coefficient smaller than δ^j is set to zero while the others remain unchanged.[11] And then the inversing wavelet transform is performed with new coefficients to reconstruct the signal characterized by a higher SNR.

The procedure flow chart of the algorithm described above is shown in Fig.1. It is implemented by a software in PC.

3 Experiments and results

In the following the WTDN described in Section 2 was used to de-noise both simulated data and sampled data, and then the poles were identified with N4SID. All data were processed again by LFDN for comparison.

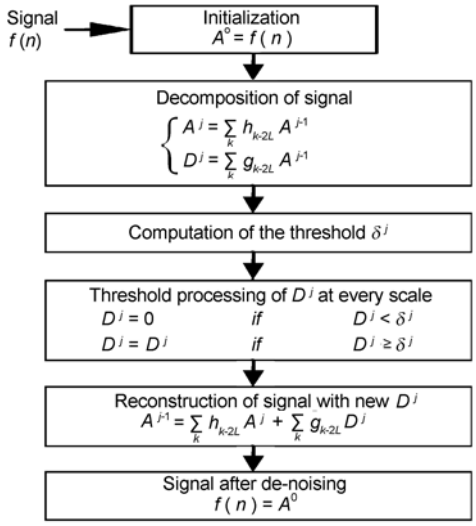

Fig.1 The procedure flow chart of the WTDN algorithm.

3.1 Estimate of simulated system

The simulated system has the following transfer function, which is similar to that of the real system,

$$F(s)=\frac{A}{(s+a_1)(s+a_2)} \tag{6}$$

where a_1=1.45×10^5, a_2=3.9×10^6, A=2.0×10^4

As usual, the "measured" impulse response is $\tilde{h}(n)=h(n)+\xi(n)$, where $h(n)$ is the "true" impulse response of $F(s)$, and $\xi(n)$ is a zero-mean Gaussian white noise ($\xi(\cdot)\approx \mathrm{WGN}(0,4.45\times10^{-4})$).

We will assume a prior estimate of $F(s)$ as

$$\overline{F}(s)=\frac{\overline{A}}{(s+\overline{a}_1)(s+\overline{a}_2)} \tag{7}$$

where $\overline{a_1}=1.6\times10^5$, $\overline{a_2}=3.0\times10^6$, $\overline{A}=2.0\times10^4$.

For $\Delta T=2.5\times10^{-8}$ second (sampling frequency of 40 MHz), the $h(n)$ and $\tilde{h}(n)$ are represented in Fig.2 (a) and (b) respectively. The N4SID method was applied to signal $\tilde{h}(n)$. Estimates of simulated system with $\tilde{h}(n)$ are illustrated in Table 1.

The impulse response $\tilde{h}(n)$ was processed by LFDN and WTDN, and the outputs $\tilde{h}_{\mathrm{LF}}(n)$ and $\tilde{h}_{\mathrm{WT}}(n)$ with higher SNR corresponding to LFDN and WTDN are obtained, respectively. The results are shown in Fig.2 (c) and (d). The N4SID method was applied to $\tilde{h}_{\mathrm{LF}}(n)$ and $\tilde{h}_{\mathrm{WT}}(n)$, and the appreciated estimates of poles for simulated system are listed in Table 1. The first 40 singular values of the extended Hankel matrices built with $\tilde{h}(n)$, $\tilde{h}_{\mathrm{LF}}(n)$ and $\tilde{h}_{\mathrm{WT}}(n)$ are displayed in Fig.3. And the results of wavelet decomposing for the impulse response $\tilde{h}(n)$ with 6 scales are shown in Fig.4.

Table 1 Estimates of poles for simulated system with data processed by different methods

Poles	True values	$\tilde{h}(n)$		$\tilde{h}_{\mathrm{LF}}(n)$		$\tilde{h}_{\mathrm{WT}}(n)$	
		Estimate	Error(‰)	Estimate	Error(‰)	Estimate	Error(‰)
a_1	145000	137750	50	143763	9	144559	3
a_2	3900000	5754768	476	3507177	101	4027204	33

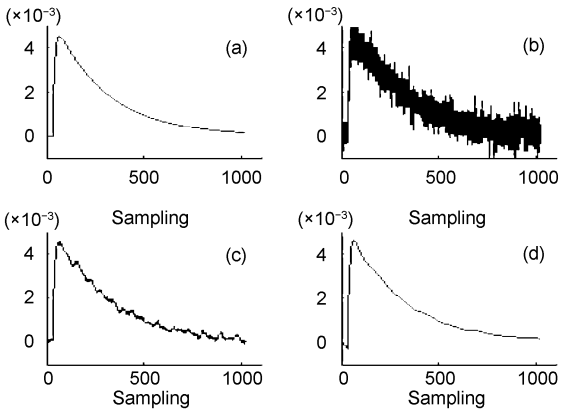

Fig.2 Impulse response of simulated system $F(s)$.
(a) Real impulse response $h(n)$, (b) Impulse response $\tilde{h}(n)$ with Gaussian white noise, (c) Output $\tilde{h}_{\mathrm{LF}}(n)$ for $\tilde{h}(n)$ de-noised by LFDN, (d) Output $\tilde{h}_{\mathrm{WT}}(n)$ for $\tilde{h}(n)$ de-noised by WTDN.

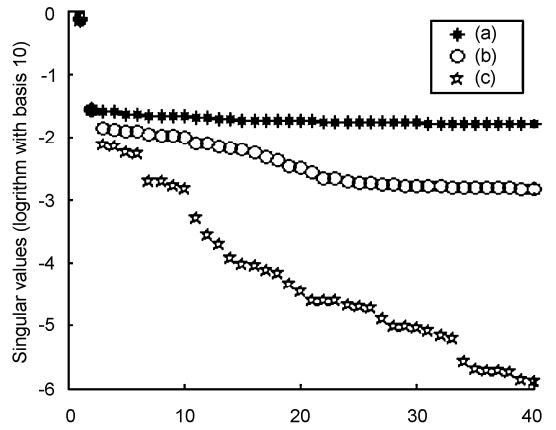

Fig.3 The first 40 singular values of the extended Hankel matrices built with impulse response of simulated system.
(a) Singular values with $\tilde{h}(n)$, (b) Singular values with $\tilde{h}_{\mathrm{LF}}(n)$, (c) Singular values with $\tilde{h}_{\mathrm{WT}}(n)$.

3.2 Estimate of actual system

Fig.5 shows the block diagram of an actual system and the signal processing chain. The sampled data are from the output of a preamplifier coupled to a gas detector at the sampling frequency of 40MHz. The original sampled data and the data de-noised by both LFDN and WTDN are displayed in Fig.6. The N4SID method was applied to the original sampled data and the data de-noised by both LFDN and WTDN. The first 40 singular values of the extended Hankel matrices built with the sampled data before and after de-noising are displayed in Fig.7. The estimates of poles for the actual system are listed in Table 2.

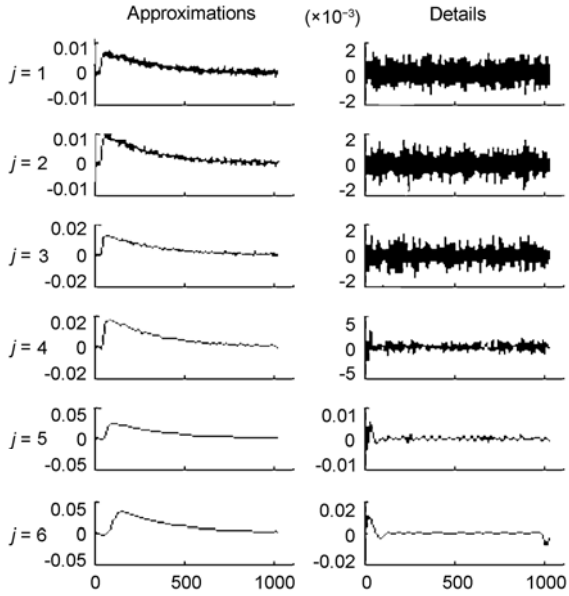

Fig.4 Wavelet decomposing for the impulse response $\tilde{h}(n)$ with 6 scales

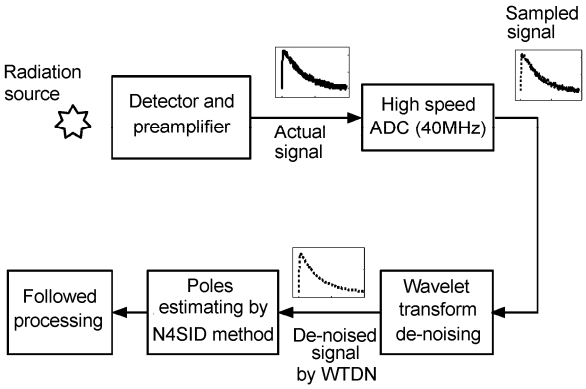

Fig.5 Block diagram of an actual system and the signal processing chain.

Table 2 Estimate of poles for a preamplifier coupled with gas detector

Poles	Estimate with the original impulse response sampled	Estimate with the impulse response de-noised by LFDN	Estimate with the impulse response de-noised by WTDN
a_1	141399	141853	141797
a_2	3876748	3958595	3946855

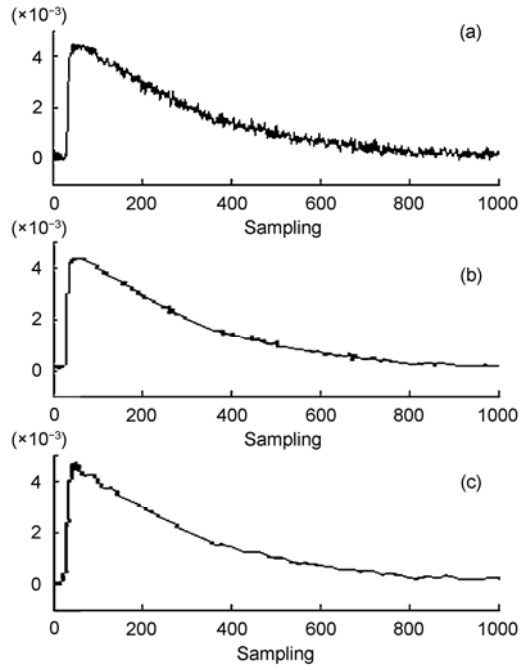

Fig.6 Impulse response sampled from the preamplifier. (a) Original impulse response sampled from the preamplifier, (b) Output for impulse response de-noised by WTDN, (c) Output for impulse response de-noised by LFDN.

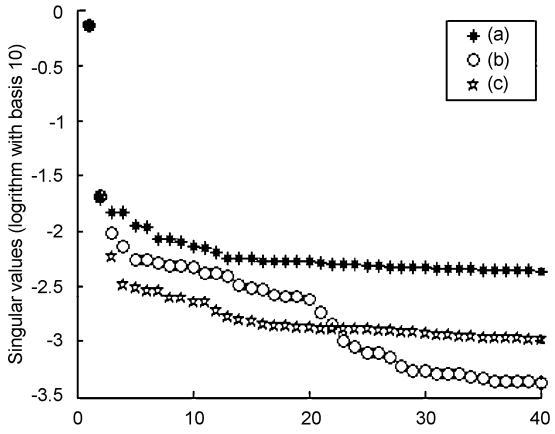

Fig.7 The first 40 singular values of the extended Hankel matrices built with impulse response of actual system (preamplifier coupled with gas detector).
(a) Singular values with the original impulse response sampled,
(b) Singular values with the impulse response de-noised by LFDN,
(c) Singular values with the impulse response de-noised by WTDN.

4 Conclusion

It is visible that the singular values of the signal (the first two singular values) are more easily distinguished from those of the noise after de-noising by WTDN than those by LFDN in Fig.3. From Table 1, the estimates of poles for simulated system are closer to the real values of $F(s)$ after de-noising than those before de-noising. The estimation accuracy preprocessed by WTDN is higher than that by LFDN. As shown in Fig.7, the signal singular values (the first two singular values) are already separated from the all of singular values after de-noising, and the difference between the signal singular values and the noise singular values is more obviously de-noised by WTDN than by LFDN. So it is reasonable to think that the sampled data de-noised by WTDN are closer to real value than those by LFDN, and the estimates of poles for the actual system corresponding to WTDN are better than that corresponding to LFDN. In Fig.8 the measured impulse response and the estimated impulse response by WTDN for the system are displayed. Notice that the overlapping is very accurate except for a little difference at the fast rising edge in the beginning of the impulse responses.

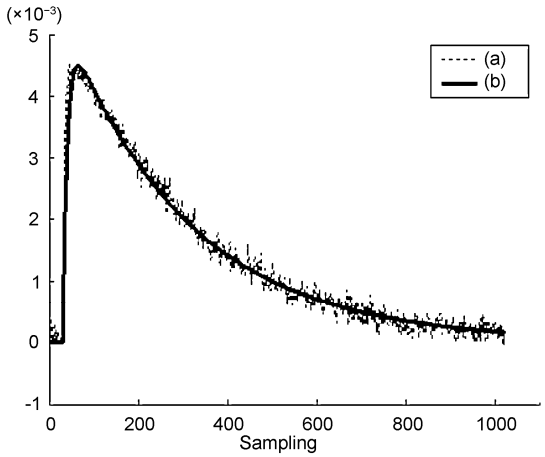

Fig.8 The measured impulse response (a) and the estimated impulse response (b).

Wavelet transform has the multiscale character. The WTDN method based on wavelet transform can improve the SNR of sampled data and the accuracy of pole identification of a system by the N4SID method. The WTDN method neither requires extra limit of the frequency range for the processed signal, nor needs a prior estimate of impulse response for identified system, so it is especially suitable to de-noise the wide-band signal and the impulse response of a blind system. The experimental results with simulated system $F(s)$ show that the estimate using N4SID with simulated data de-noised by WTDN is better than that by LFDN, which indicates that the WTDN method is reliable and available. The experimental results in the actual system (preamplifier coupled with gas detector) validate that the WTDN method is very useful for improving the SNR of sampled data, which can help to enhance the accuracy in pole identifications for an identified system with the N4SID method.

References

1 Bolić M, Drndarević V. Nucl Instr Meth, 2002, **A482**: 761-766

2 Cardoso J M R, Simőes J B, Correia C M B. Nucl Instr Meth, 1999, **A422**: 400-404

3 Geraci A, Zambusi M, Ripamonti G. IEEE Trans Nucl Sci, 1996, **43** (2): 731-736

4 Los Arcos J M, García-Toraňo E, Olmos P *et al*. Nucl Instr Meth, 1994, **A353**: 251-253

5 Overschee P V, de Moor B. Automatica, 1994, **30** (1): 75-93

6 Bittanti S, Gatti E, Ripamonti G *et al*. IEEE Trans Nucl Sci, 1997, **44** (2): 125-133

7 Bittanti S, Gatti E, Ripamonti G *et al*. IEEE Trans Contr Sys Tech, 2000, **8** (1): 127-137

8 Daubechies I. IEEE Trans Inform Theory, 1990, **36** (5): 961-1005

9 Mallat S G. IEEE Trans PSMI, 1989, **11** (7): 674-693

10 Mallat S G. IEEE Trans ASSP, 1989, **37**: 2091-2110

11 Donoho D L. IEEE Trans Inform Theory, 1995, **41**: 613-627

12 Mallat S G. IEEE Trans Inform Theory, 1992, **38** (2): 617-643